Elevated ozone events over Johannesburg based on analysis of tropospheric ozone partial columns

Atham Raghunandan[a,b], Gilberto Mahumane[b,c] and Roseanne Diab[b*]

Traditionally, tropospheric column ozone (TCO) is a useful indicator for comparing both temporal and spatial variations in tropospheric ozone. TCO variations over Johannesburg are analysed in this paper with a view to identifying days of enhanced ozone, which could then form the basis of a detailed investigation to determine sources of the elevated ozone. We used ozone data from the Measurement of Ozone and Water Vapor by Airbus In-Service Aircraft (MOZAIC) database for the period 1995 to 1998. A fixed tropopause height of 12 km was employed in this analysis as the upper bound of the troposphere. Seasonal and inter-annual variations in TCO provided a context for this study. A clear seasonal cycle exists, with TCO peaking in September and October. Minimum TCO occurs in autumn, when variability is also least. The lower day-to-day variability in autumn and winter is a reflection of the more settled weather at this time. This period is representative of background tropospheric ozone loadings, on which the dynamic and photochemical influences of other months are superimposed. High-TCO events, defined as exceeding 30 DU (Dobson units), occurred predominantly in spring. Enhancements in the lower troposphere are shown to be generally short-lived (1–2 days) and due to the effects of local surface pollution sources, and arise most likely from biomass burning, which peaks in spring. In contrast, events in the upper troposphere prevailed for a longer period and were due to the penetration of ozone-rich air from the stratosphere, as shown in a case study in September 1998.

Introduction

Tropospheric column ozone (TCO) is defined as the integrated amount of ozone in a vertical column of air between the earth's surface and the tropopause. It is measured in Dobson units (DU), where 1 DU is 2.687×10^{16} molecules per square centimetre of the column cross section. A fixed tropopause height of 12 km was assumed in this analysis as the upper bound of the troposphere.

TCO provides a useful way to compare the temporal and spatial distribution of tropospheric ozone and its variability in different geographical locations[1] and to detect seasons of enhanced ozone.[2–7] As an integrated measure, it effectively overcomes the problem of trying to compare vertical profiles, in which ozone enhancements occur at greatly different altitudes. It has also been helpful in the validation of satellite data, in which comparisons of ground-based and tropospheric residuals inferred from TOMS (Total Ozone Mapping Spectrometer) satellite-based measurements of TCO have been made[6–8] to determine the relative accuracy of measurements. In all cases, a high level of agreement was found.

Previous studies of TCO over South Africa[2,9] investigated the seasonal and inter-annual variability of integrated tropospheric ozone over Irene (25°52′S, 28°13′E, 20 km southeast of Pretoria) during the SAFARI-92 (Southern African Fire–Atmosphere Research Initiative) field campaign. Irene exhibited a general springtime (September–October) enhancement. According to these studies,[2,9] the seasonal peak appeared to be a reflection of the seasonal burning pattern over Africa detected by satellite.[10] This was confirmed by subsequent studies which showed that southern Africa was supplied with abundant precursors from biomass burning, biogenic emissions and lightning,[11] which re-circulated within the stable anticyclonic circulation.[12] The conclusion was that both the dynamics of the region (high ozone formation rates, extensive recirculation and stable layering) and the multiple diverse sources played an important role in ozone build-up.[2,9,11] TCO is used in this paper to identify days of enhanced ozone with a view to understanding the origins of such elevated events.

Data and methods

Ozone and meteorological profile data over Johannesburg (26°10′S, 28°01′E) for the period 1995 to 1998 were used to estimate TCO. The data were derived from the Measurement of Ozone and Water Vapor by Airbus In-Service Aircraft (MOZAIC) database, generated by continuous-measuring equipment installed on five in-service Airbus A340 aircraft. The MOZAIC programme, which was launched in 1993, aims to collect reliable, high-quality experimental data, to help understand the changing composition of the atmosphere as a consequence of human activity.[13]

The ozone analyser used is a dual-beam UV absorption instrument (Thermo-Electron, Model 49-103), with a precision of 2 ppbv (parts per billion by volume), minimum detection limit of 2 ppbv and an accuracy of 2%. Instrument calibration and data verification techniques have been described in detail by Thouret *et al.*[14] This ozone analyser has a response time of 4 seconds, providing a vertical resolution of approximately 30 m (during ascent and descent). These raw data are averaged over 150-m vertical depth layers along the vertical tropospheric column.[15]

A total of 381 profiles was finally selected from the 427 ozone profiles that were available for Johannesburg over the period 1995–1998 for the computation of TCO. The remaining 46 were discarded because of continuous missing data over a vertical distance that exceeded 1050 m. This distance was arbitrarily selected as approximately 1000 m, and was equivalent to seven 150-m layers. Data were interpolated from the mean monthly profile, if the height interval(s) over which data were missing was less than 1050 m.

A measure of TCO was obtained by integrating the averaged ozone profiles between the surface (sfu) and a predetermined height of 12 km (above sea level). The method used to compute integrated TCO (or the column ozone amount in the troposphere) is based on ozone readings in ppbv at available levels. The conversion to DU at each level was estimated as follows:

$$O_{DU} = \left(\frac{(O_{ppbv} / 10^{-9}) \times p \times \Delta H \times 273.15 \times 1000}{1013.25 \times T_K} \right) \times 100 ,$$

where O_{ppbv} = ozone concentration (ppbv), O_{DU} = ozone in Dobson units, T_K = temperature (K), ΔH = {[Difference in height between 2 successive layers (geopotential metres)]/2}, and p = pressure (hPa).

TCO was subsequently subdivided into four layers within the

[a]Present address: CSIR Natural Resources and the Environment, P.O. Box 17001, Congella 4013, South Africa. E-mail: araghunandan@csir.co.za

[b]School of Environmental Sciences, University of KwaZulu-Natal, Howard College Campus, Durban 4041, South Africa.

[c]On study leave from Department of Physics, Eduardo Mondlane University, Maputo, Mozambique.

*Author for correspondence. E-mail: diab@ukzn.ac.za

troposphere, namely, sfc–3 km, 3–5, 5–7 and 7–12 km, in order to investigate the factors responsible for TCO variations. The layers were selected on the basis of the work of Cosijn and Tyson[16] on absolutely stable layers over southern Africa, which occur preferentially at approximately 700 hPa (3 km), 500 hPa (5 km) and 300 hPa (7 km).

Various methods exist for determining the upper level below which ozone may be integrated. Ideally, this height should represent the tropopause, which is known to vary on a seasonal[17,18] and a daily basis. Some studies define a dynamic tropopause that is based on a change in potential vorticity (PV).[19,20] Others define a thermal tropopause based on the vertical temperature gradient.[21] Yet others define a chemical tropopause that is based on the height at which ozone shows a sudden increase.[22] Related to this last approach is one in which an ozone threshold of 100 ppbv was used to distinguish stratospheric air from tropospheric air.[11,23,24]

A fixed altitudinal upper limit was used in this paper because 12 km is the flying altitude reached by the MOZAIC aircraft, in accordance with air traffic regulations. TCO values are thus expected to be less than those estimated previously for Irene,[2,9,11] where an upper limit of 15 km could be used, as estimates were derived from ground-based ozonesonde data. While actual magnitudes may differ between the studies, seasonal trends are expected to be comparable, and the intention to detect days of relatively enhanced ozone is not compromised.

The case study discussed in the paper relied not only on MOZAIC profile data but also on ozone and meteorological transect data, collected during a MOZAIC flight at cruise altitude from Johannesburg to Cape Town (33.93°S, 18.45°E). Additional meteorological data from the European Centre for Medium Range Weather Forecasting (ECMWF) were also used, to provide supporting evidence for some of the features observed.

Results

Seasonal and inter-annual variations in tropospheric column ozone

Figure 1 shows that mean TCO values at Johannesburg are highest during September and October (~32 DU) and lowest in autumn (~18 DU), confirming the seasonal pattern that has been noted by many authors[2,25–28] for Irene. Indeed, the pattern is a well-established southern hemisphere trend and has also been observed at Réunion (21°S, 55°E),[29] Natal in Brazil (5°25′S, 35°23′E),[6] Okaukuejo in Namibia (19°11′S, 15°55′E),[2] Ascension Island (8°S, 14°E)[7] and Brazzaville (4°17′S, 15°16′E).[30] Most studies have suggested that the main reason for this spring maximum is biomass burning in combination with prevailing subtropical anticyclonic circulation patterns over southern Africa.[2,9] According to Diab *et al.*,[2] the extension of the ozone enhancement into summer over Irene, also evident over Johannesburg (Fig. 1), indicates a local urban-industrial source, as was first suggested by Zunckel *et al.*[25] The mean annual range in TCO is 14.9 DU, which is consistent with that derived for Irene, namely, ~13 DU.[9]

Day-to-day fluctuations in TCO, expressed by the magnitude of the standard deviation bars (Fig. 1), show highest variability in January, September and November, each with a standard deviation of ~4.5 DU, and least during autumn and winter (April to July), when the standard deviation is in the range 2.3–2.5 DU. The lower day-to-day variability in autumn and winter is attributable to the dominance of the subtropical anticyclonic circulation and consequently more settled weather at this time.

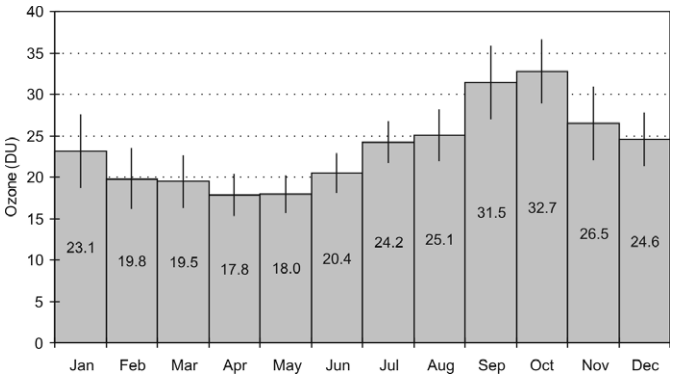

Fig. 1. Mean monthly TCO (DU) above Johannesburg for the period 1995–1998, based on MOZAIC aircraft data. The vertical bars indicate one standard deviation on either side of the mean.

Seasonal forcing is well developed and consistent from year to year. Inter-annual variability in TCO (not shown here but presented elsewhere[31]) is minimal between April and June, again indicating that these months represent background tropospheric ozone loadings on which the dynamic and photochemical influences of other months are superimposed. Inter-annual variability is greater at other times of the year, but mean monthly values seldom differ by more than 5 DU from year to year.

Integrated tropospheric ozone in layers

Integrated tropospheric ozone in each of four layers reveals the same spring maximum in each layer (Fig. 2). Below 5 km, the TCO minimum occurs in February and March, whereas above 5 km, the minimum is evident in April and May. These results suggest a decoupling of the atmosphere and emphasize the important role of the 5 km absolutely stable layer in the accumulation and dispersal of atmospheric pollutants. Indeed, Tyson *et al.*[32] drew attention to its persistence, effectively preventing the vertical transport of pollutants, and trapping pollution between intervening stable layers. The seasonal cycle is particularly well developed in the 7–12 km layer.

The percentage increase observed in each of the other months was computed taking the months of February and March for layers below 5 km, and April and May for layers above 5 km, as representative of background ozone loadings. In each case, the greatest enhancement occurred in October, with values of 143% in the sfc–3 km layer, 96% in the 3–5 km layer, 103% in the 5–7 km layer, and 100% in the 7–12 km layer. The October enhancement thus occurs throughout the troposphere. It is not possible to distinguish between surface-based photochemical production and subsequent transport to higher layers, on the one hand,

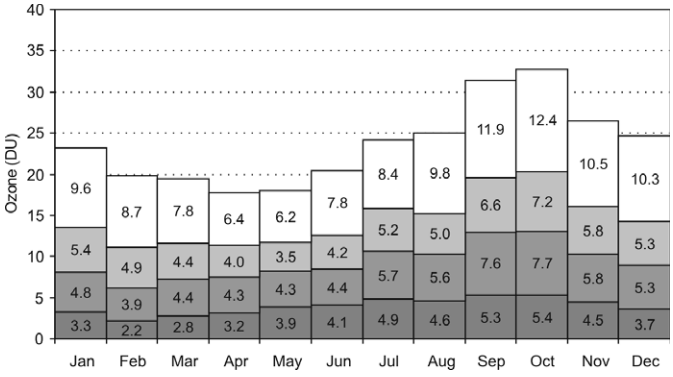

Fig. 2. Monthly integrated TCO layers for 1995–1998. Dark grey = sfc–3 km; grey = 3–5 km; light grey = 5–7 km; white = 7–12 km layers.

and upper tropospheric dynamical sources and subsequent transport to lower layers on the other.

Elevated ozone events

A further analysis of days with highest TCO was undertaken to obtain greater insight into factors responsible for ozone enhancement. A threshold value of 30 DU was arbitrarily selected to mark an event of considerable ozone enhancement. This threshold was previously used for a similar study over Irene,[2] whereas Thompson *et al.*[11] adopted a value of 35 DU.

Figure 3 presents the breakdown of TCO into layers for individual days on which TCO exceeded 30 DU. High-TCO events occurred predominantly during September (16 events) and October (17), with the few remaining events scattered throughout the year. The percentage contribution of each layer to TCO on a particular day was compared with the mean percentage contribution of each layer, enabling layers of enhancement to be identified for individual days. In the lower troposphere, 22 events showed enhancements in the sfc–3 km layer, 23 in the 3–5 km layer, and

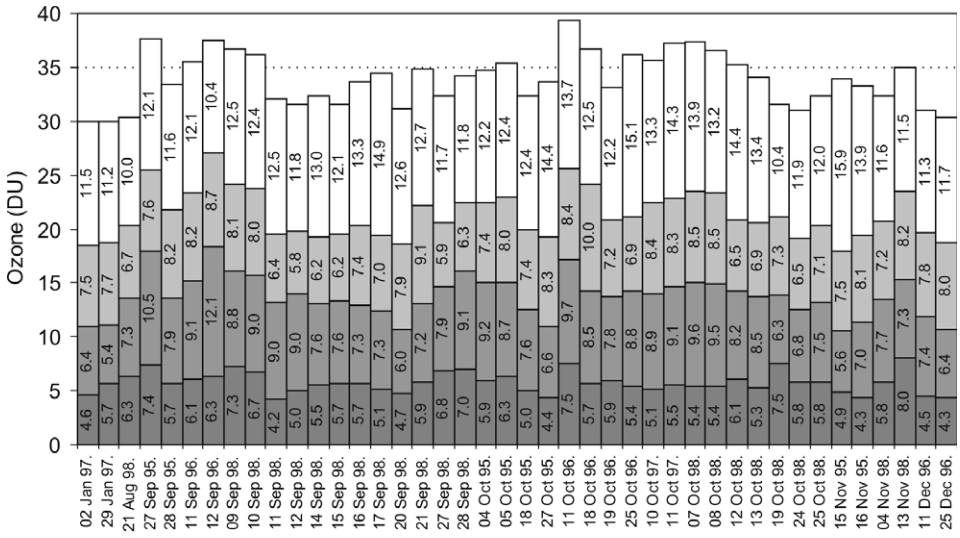

Fig. 3. Ozone events with TCO greater than 30 DU. Dark grey = sfc–3 km; grey = 3–5 km; light grey = 5–7 km; white = 7–12 km layers.

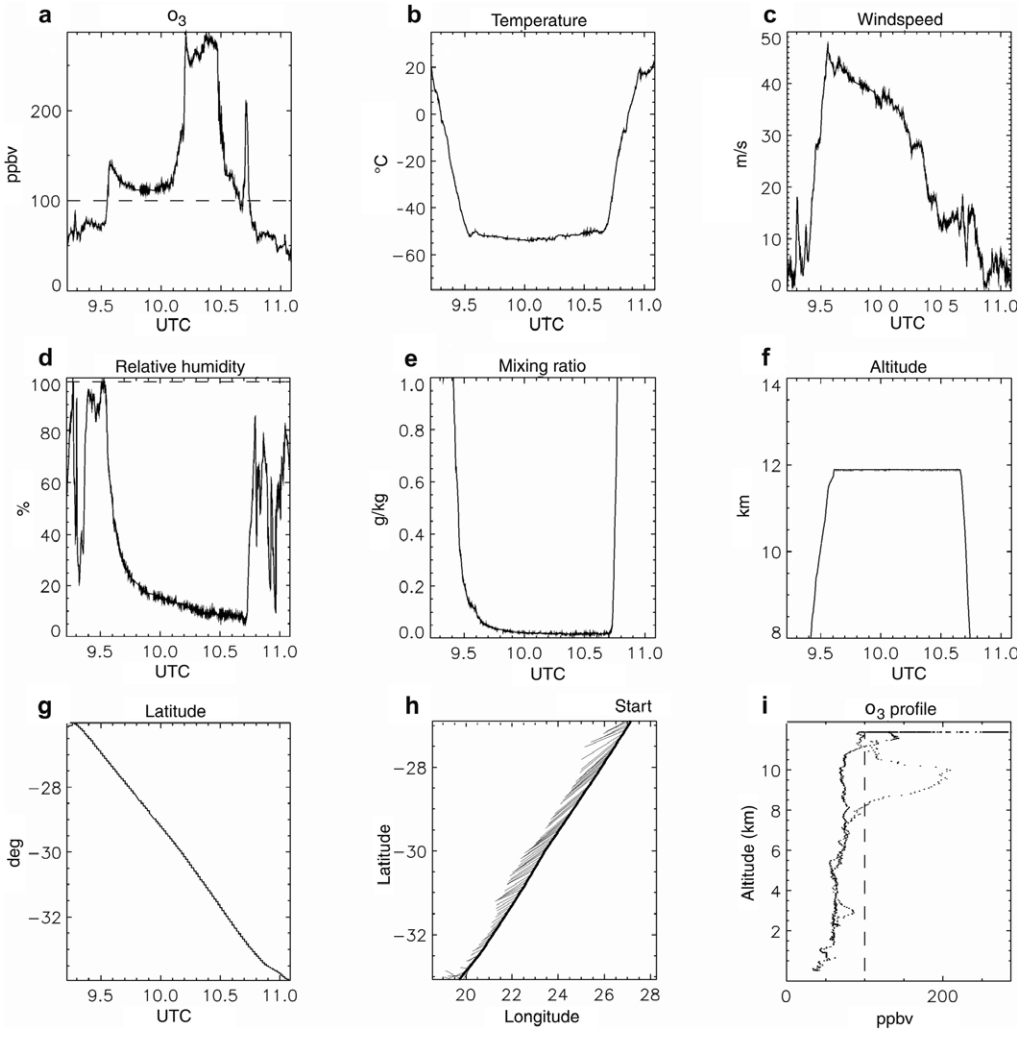

Fig. 4. MOZAIC flight parameters for a flight on 16 September 1998. Time series (decimal hours) of: **a**) ozone mixing ratio (ppbv); **b**) temperature (°C); **c**) wind speed (m s^{-1}); **d**) relative humidity (%); **e**) water vapour mixing ratio (g kg^{-1}); **f**) aircraft altitude (km); **g**) latitude (degrees); **h**) wind vectors ending along the aircraft flight path on a latitude–longitude plan.; **i**) ozone profile (ppbv) during ascent (solid line) and descent (dotted line).

13 events manifested elevated ozone in both layers. These enhancements seldom lasted for more than 1–2 consecutive days and occurred mostly in September. These events are ascribed to effects of local surface pollution sources, most likely biomass burning rather than urban-industrial effects, because the enhancement is dominant in spring rather than spread throughout the year. Previous studies of the incidence of biomass burning over southern Africa have confirmed this springtime maximum.[10]

The number of events showing enhancements in the mid- and upper troposphere was similar: 20 in the 5–7 km layer and 21 in the 7–12 km layer. An extended period of enhancement occurred in the 7–12 km layer from 14–17 September 1998 and again on 20 September 1998 (Fig. 3). In view of the extended duration of this event, it was selected for further detailed investigation, to determine the origin of the elevated ozone. Full details of this ozone event are given elsewhere.[33]

Case study of a high-ozone event

Data from a MOZAIC flight between Johannesburg and Cape Town on 16 September 1998 are presented in Fig. 4 as time series plots of various MOZAIC parameters. For much of the flight, ozone mixing ratios were above 100 ppbv, this value being a commonly used threshold[14,23] to indicate ozone-rich stratospheric air (Fig. 4a). A maximum value of 287 ppbv was recorded at 10.21 UTC at 30.14°S (Figs 4a, g). Two further secondary ozone peaks are evident; one of 141 ppbv at 9.6 UTC at an altitude of 11.5 km, shortly before the aircraft reached its cruise altitude, and a second of 209 ppbv at 10.71 UTC, recorded during descent over Cape Town (Figs 4a, f).

This high-ozone event occurred in association with relative humidity values of less than 20% (Fig. 4d) and very low water vapour mixing ratio values (Fig. 4e). Temperatures were of the order of –50°C (Fig. 4b). Wind speeds at the time of the first ozone peak exceeded 40 m s^{-1} (Fig. 4c) and were strong westerly to southwesterly along the entire flight path (Fig. 4h). The vertical ozone profiles recorded during ascent over Johannesburg and descent over Cape Town reveal the presence of an elevated enriched ozone layer (up to 200 ppbv) extending between approximately 8 and 10 km over the coastal city (Fig. 4i).

Plots of ECMWF geopotential height data on various pressure surfaces for 16 September 1998 over the southern African subcontinent and adjacent oceans showed a westerly wave that had passed over the subcontinent and was subsequently situated east of it (it was located at ~35°S, 45°E on the 250 hPa surface).[38] Consequently, most of southern Africa is characterized by strong westerly winds, weakening to southwesterlies closer to Cape Town. This is consistent with aircraft measurements shown in Figs 4c and 4f along the aircraft flight path. ECMWF-analysed wind speeds also clearly depict the westerly subtropical jet stream over the subcontinent, with wind speeds exceeding 40 m s^{-1} (Fig. A in supplementary material online).

PV values on the 335 K and 345 K isentropic surfaces range from –1 to –2 PVU, which are intermediate between tropospheric and stratospheric values, and increase towards the south (become more negative) to reach stratospheric values (above an absolute value of 2 PVU) over the southern latitudes of the continent.

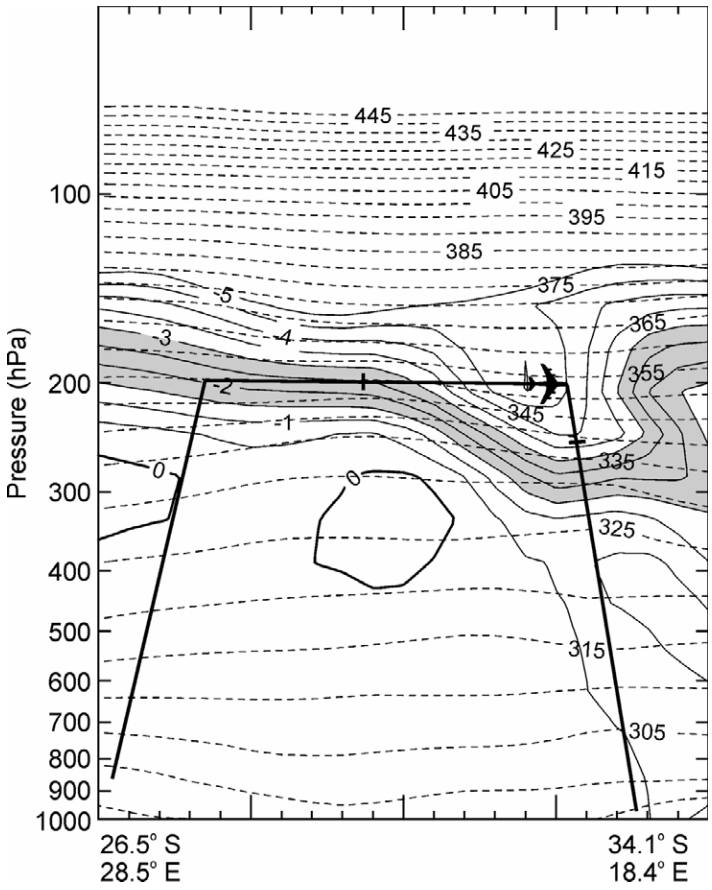

Fig. 5. Vertical cross section of potential vorticity (PV) along the aircraft flight path (contour interval 0.5 PVU, values between 1.5 and 3.0 PVU are shaded) and potential temperature (contour interval 5 K) at 0600 UTC on 16 September 1998 (the aircraft flight path is indicated by a thick line)

A vertical cross section of PV derived from 06:00 UTC ECMWF data along the aircraft flight path is shown in Fig. 5. A tropopause deformation is evident, and it is deflected in a southwesterly direction, in which PV values greater than an absolute value of 3 PVU are transported below 250 hPa, clearly linking the ozone episode with air of stratospheric origin.

The association between enhanced ozone, dry air and high PV confirms that air has been brought down from higher altitudes in the stratosphere to the upper troposphere. This ozone enhancement is likely to be associated with the subtropical jet and baroclinic westerly wave development referred to earlier. Much of the ozone transport from the lower stratosphere into the troposphere is ascribed to tropopause deformation. The most extensive tropopause folding occurs in association with baroclinic waves linked to strong jet streams.[34,35] Both an upper-level westerly wave over the southern Indian Ocean and a strong subtropical jet over southern Africa are indicated as having been present at this event.

Conclusion

TCO was used in this study to identify elevated ozone events, defined as having a TCO value greater than 30 DU, over Johannesburg. Seasonal and inter-annual variations in TCO provided a context for the study. The seasonal pattern in TCO, dominated by a spring maximum and autumn minimum, was confirmed by this study. Seasonal forcing is consistent from year to year, with TCO peaking either in September or October. The integration of tropospheric ozone in layers has provided some insights into the factors responsible for TCO variations. Below 5 km, the TCO minimum occurred in February and March,

whereas above 5 km, the minimum was in April and May. These results endorse a decoupling of the atmosphere, and emphasize the role of the 5 km absolutely stable layer.

Elevated TCO events occurred predominantly during September and October. Enhancements in the lower troposphere are most likely due to effects of local surface pollution sources, such as biomass burning because the maximum was restricted to springtime. Such events were characteristically short-lived, 1–2 days, whereas those in the upper troposphere (7–12 km layer) extended over longer periods. A case study analysis for 16 September 1998 revealed evidence of stratospheric–tropospheric exchange as a result of tropopause folding in association with a baroclinic westerly wave linked to a strong jet stream.

In conclusion, we attribute ozone enhancements in spring to both localized low-level sources such as biomass burning, as well as upper tropospheric sources such as exchange of ozone-rich air from the stratosphere.

Frank Sokolic is thanked for assistance with the computation of TCO. Participating airlines (Lufthansa, Air France, Sabena and Austrian) and European funding of MOZAIC-III (Contract EVK2-CT-1999-00015) are acknowledged. The National Research Foundation is thanked for providing student support and the CSIR Young Researcher Establishment Fund is acknowledged for co-funding.

Received 19 March. Accepted 26 June 2007.

1. Zbinden R.M., Cammas J-P., Thouret V., Nédélec P., Karcher F. and Simon P. (2006). Mid-latitude tropospheric ozone columns from the MOZAIC program: climatology and interannual variability. *Atmos. Chem. Phys. Discuss.* **6**, 1053–1073.
2. Diab R.D., Thompson A.M., Zunckel M., Coetzee G.J.R., Combrink J., Bodeker G.E., Fishman J., Sokolic F., McNamara D.P., Archer C.B. and Nganga D. (1996). Vertical ozone distribution over southern Africa and adjacent oceans during SAFARI-92. *J. Geophys. Res.* **101**(D19), 23823–23833.
3. Logan J.A. (1985). Tropospheric ozone: seasonal behavior, trends, and anthropogenic influence. *J. Geophys. Res.* **90**(D6), 10463–10482.
4. Olson J.R., Fishman J., Kirchhoff V.W.J.H. Nganga D. and Cros B. (1996). Analysis of the distribution of ozone over the southern Atlantic region. *J. Geophys. Res.* **101** (D19), 24083–24093.
5. Oltmans S.J., Galbally I.E., Brunke E-G., Meyer C.P., Lathrop J.A., Johnson B.J., Shadwick D.S., Cuevas E., Schmidlin, F.J., Tarasick D.W., Claude H., Kerr J.B., Uchino O. and Mohnen V. (1998). Trends of ozone in the troposphere. *Geophys. Res. Lett.* **25**(2), 139–142.
6. Thompson A.M., Witte J.C., McPeters R.D., Oltmans S.J., Schmidlin F.J., Logan J.A., Fujiwara M., Kirchhoff V.W.J.H., Posny F., Coetzee G.J.R., Hoegger B., Kawakami S., Ogawa T., Johnson B.J., Vömel H. and Labow G. (2003). Southern Hemisphere Additional Ozonesondes (SHADOZ) 1998–2000 tropical ozone climatology 1. Comparison with Total Ozone Mapping Spectrometer (TOMS) and ground-based measurements. *J. Geophys. Res.* **108**(D2), 10-1–10-19.
7. Thompson A.M. and Hudson R.D. (1999). Tropical tropospheric ozone (TTO) maps from Nimbus 7 and Earth Probe TOMS by the modified-residual method: evaluation with sondes, ENSO signals, and trends from Atlantic regional time series. *J. Geophys. Res.* **104**(D21), 26961–26975.
8. Cros B., Nganga D., Minga A., Fishman J. and Brackett V. (1992). Distribution of tropospheric ozone at Brazzaville, Congo, determined from ozonesonde measurements. *J. Geophys. Res.* **97**(D12), 12869–12875.
9. Thompson A.M., Diab R.D., Bodeker G.E., Zunckel M., Coetzee G.J.R., Archer C.B., McNamara D.P., Pickering K.E., Combrink J., Fishman J. and Nganga D. (1996). Ozone over southern Africa during SAFARI-92/TRACE A. *J. Geophys. Res.* 101(D19), 23793–23807.
10. Cahoon D.R., Stocks B.J., Levine J.S., Cofer W.R. and O'Neill K.P. (1992). Seasonal distribution of African savanna fires. *Nature* **359**, 812–815.
11. Thompson A.M., Pickering K.E., McNamara D.P., Schoeberl M.R., Hudson R.D., Kim J.H., Browell E.V., Kirchoff V.W.J.H. and Nganga D. (1996b). Where did tropospheric ozone over southern Africa and the tropical Atlantic come from in October 1992? Insights from TOMS, GTE TRACE A, and SAFARI 1992. *J. Geophys. Res.* **101**, 24251–24278.
12. Garstang M., Tyson P.D., Swap R., Edwards M., Kållberg P. and Lindesay J.A. (1996). Horizontal and vertical transport of air over southern Africa. *J. Geophys. Res.* **101**(D19), 23721–23736.
13. Marenco A., Thouret V., Nedélec P., Smit H., Helten M., Kley D., Karcher F., Simon P., Law K., Pyle J., Poschmann G., Wrede R.V., Hume C. and Cook T. (1998). Measurement of ozone and water vapour by Airbus in-service aircraft: the MOZAIC airborne program, an overview. *J. Geophys. Res.* **103**(D19), 25631–25642.
14. Thouret V., Marenco A., Nedélec P. and Grouhel C. (1998). Ozone climatologies at 9–12 km altitude as seen by the MOZAIC airborne program between September 1994 and August 1996. *J. Geophys. Res.* **103**(D19), 25653–25679.
15. MOZAIC-II: Technical Final Report (1996–1999) (2000). January 2000. University of Paul Sabatier, Toulouse, France.
16. Cosijn C. and Tyson P.D. (1996). Stable discontinuities in the atmosphere over South Africa. *S. Afr. J. Sci.* **92**, 381–386.
17. Reiter E.R. (1975). Stratospheric-tropospheric exchange processes. *Rev. Geophys. Space Phys.* **13**(4), 459–473.
18. Staley D.O. (1962). On the mechanism of mass and radioactivity transport from the stratosphere to troposphere. *J. Atmos. Sci.* **19**, 450–467.
19. Danielsen E.F. (1968). Stratospheric-tropospheric exchange based on radioactivity, ozone and potential vorticity. *J. Atmos. Sci.* **25**, 502–518.
20. Reed R. (1955). A study of a characteristic type of upper-level frontogenesis. *J. Meteorol.* **12**, 226–237.
21. World Meteorological Organisation (WMO) (1986). *Atmospheric ozone.* Report 36, Geneva.
22. Bethan S., Vaughan G. and Reid S.J. (1996). A comparison of ozone and thermal tropopause heights and the impact of tropopause definition on quanfying the ozone content of the troposphere. *Q. J. R. Met. Soc.* **122**, 929–944.
23. Cammas J-P., Jacoby-Koaly S., Suhre K., Rosset R. and Marenco A. (1998). Atlantic subtropical potential vorticity barrier as seen by Measurements of Ozone by Airbus In-Service Aircraft (MOZAIC) flights. *J. Geophys. Res.* **103** (D19), 25681–25693.
24. Thompson A.M., Witte J.C., Oltmans S.J., Schmidlin F.J., Logan J.A., Fujiwara M., Kirchoff V.W.J.H., Posny F., Coetzee G.J.R., Hoeger B., Kawakami S., Ogawa T., Fortuin J.P.F. and Kelder H.M. (2003). Southern Hemisphere Additional Ozonesondes (SHADOZ) 1998–2000 tropical ozone climatology. 2, Tropospheric variability and the zonal wave-one. *J. Geophys. Res.* **108**(D2), 8241–8262.
25. Zunckel M., Diab R.D. and Scourfield M.W.J. (1992). Vertical distribution of ozone at Pretoria: comparisons between 1965–68 and 1990–1991. *The Clean Air J.* **8**, 3–8.
26. Combrink J., Diab R.D., Sokolic F. and Brunke E.G. (1995). Relationship between surface, free tropospheric and total column ozone in two contrasting areas in South Africa. *Atmos. Environ.* **29**(6), 685–691.
27. Diab R., Barsby J., Bodeker G., Scourfield M. and Salter L. (1992). Satellite observations of total ozone above South Africa. *S. Afr. Geog. J.* **74**, 13–18.
28. Diab R.D., Thompson A.M., Mari K., Ramsay L. and Coetzee G.J.R. (2004). Tropospheric ozone climatology over Irene, South Africa from 1990–1994 and 1998–2001. *J. Geophys. Res.* **109**, D20301, doi:10.1029/2004JD004793, 2004.
29. Baldy S., Ancellet G., Bessafi M., Badr A. and Lan Sun Luk D. (1996). Field observations of the vertical distribution of tropospheric ozone at the island of Réunion (southern tropics). *J. Geophys. Res.* **101**(D19), 23835–23849.
30. Nganga D., Minga A., Cros B., Bouka Biona C., Fishman J. and Grant W.B. (1996). Ozone over southern Africa during SAFARI-92/TRACE A. *J. Geophys. Res.* **101**(D19), 24095–24103.
31. Raghunandan A. (2003). *Nature and characteristics of tropospheric ozone over Johannesburg.* M.A. thesis, University of Natal, Durban.
32. Tyson P.D., Garstang M., Thompson A.M., Diab R.D., Browell E.V. and D'Abreton P.C. (1997). Correspondence between ozone measurements, transport and production of ozone over south central Africa. *J. Geophys. Res.* **102**(D9), 10623–10636.
33. Mahumane G. (2002). *Analysis of high ozone events over Africa.* M.Sc. thesis, Univerisity of Natal, Durban.
34. Holton J.R., Haynes P.H., McIntire M.E., Douglass A.R., Rood R.B. and Pfister L. (1995). Stratospheric-tropospheric exchange. *Rev. Geophys.* **33**, 403–439.
35. Baray J.L., Ancellet G., Taupin F.G., Bessafi M., Baldy S. and Keckhut P. (1998). Subtropical tropopause break as a possible stratospheric source of ozone in the tropical troposphere. *J. Atmos. Sol.-Terr. Phys.* **60**, 27–36.

This article is accompanied by supplementary material online at www.sajs.co.za

Supplementary material to:

Raghunandan A., Mahumane G. and Diab R. (2007). Elevated ozone events over Johannesburg based on analysis of tropospheric ozone partial columns. *S. Afr. J. Sci.* **103**, 248–252.

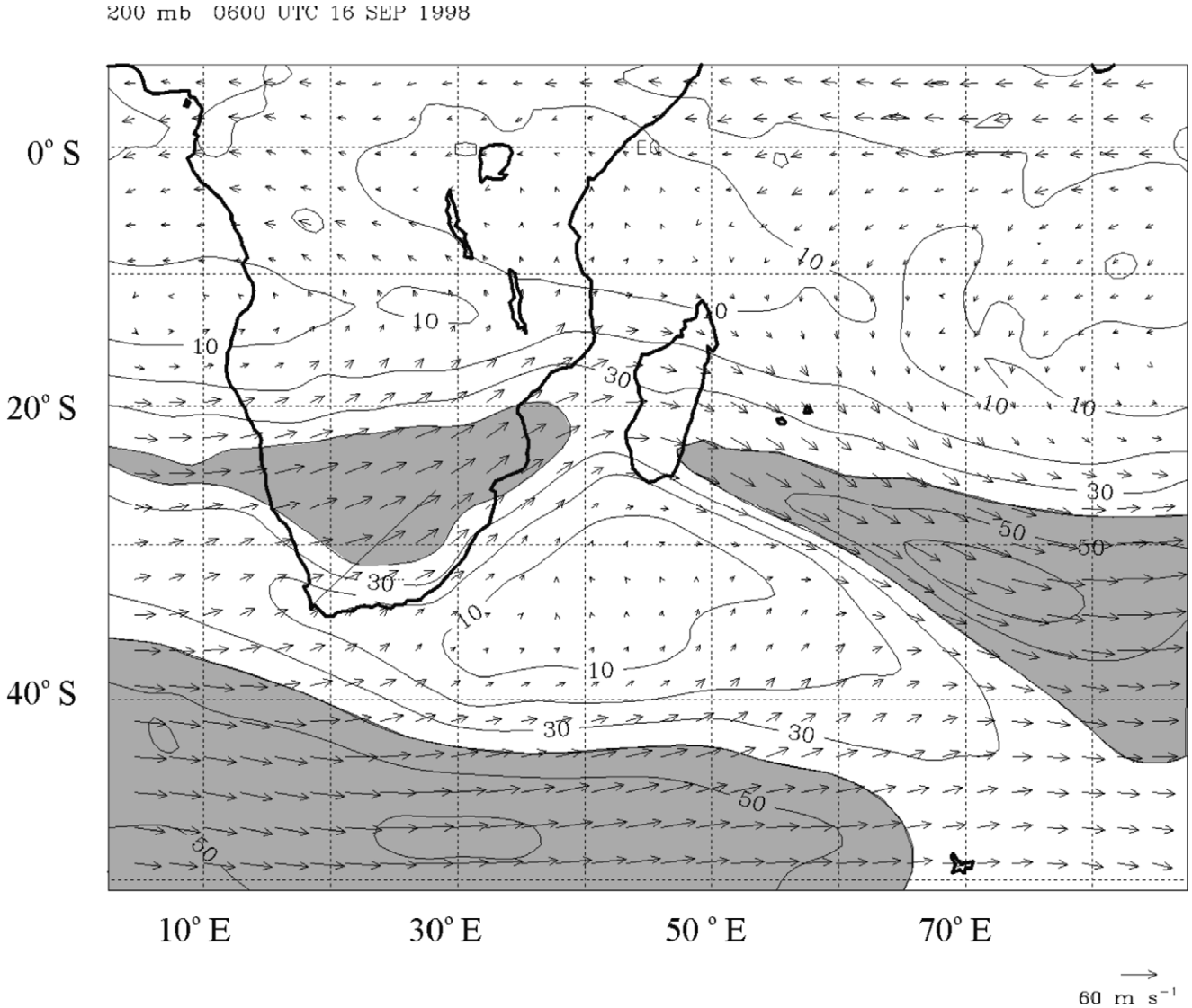

Fig. A. ECMWF-analysed wind speeds (contour interval 10 m s ^{1}, values greater than 40 m s ^{1} are shaded) and wind vectors on the 200 hPa surface on 16 September 1998, at 06:00 UTC.